SPINNING CONES AS PUMPS, DEGASSERS AND LEVEL CONTROLLERS

M. Cooke[1], P.J.Heggs[1], A. Eaglesham[2] and and D. Housley[3]

[1]Dept. of Chemical Engineering, UMIST, PO Box 88, Manchester, M80 1QD, UK
E-mail: michael.cooke@umist.ac.uk, p.j.heggs@umist.ac.uk

[2]Huntsman Polyurethanes, 3078 Everburg, Belgium.
E-mail: archie_eaglesham@huntsman.com

[3]DuPont (UK) Limited, DuPont Polyester Technologies, PO Box 2002,Wilton, Middlesborough, TS90 8JF. E-mail: duncan.housley@gbr.dupont.com

The literature on spinning cones as pumps and degassers is reviewed. Experiments on a spinning cone rig designed to measure spinning cone-pumping rates are described. A large number of experiments were carried out, measuring pumping rates as a function of cone angle and immersion depth. Cone half angles were from 15 to 60 degrees. Most of the tests were done with water but a number of runs were carried out with 75% by volume glycerol solution. This changed the viscosity and fluid density. An equation is proposed to predict the volumetric pumping rate (Q) of a cone in terms of its geometry and the physical properties of the fluids.

Experiments with gassed fluids indicate that the liquid pumping rate of a spinning cone is independent of any gas present. It was also found that both outside and inside surfaces of the cone contribute equally to the fluid pumping process.

The effectiveness of spinning cones as a degasser and/or level controller have been tested in mechanically agitated baffled vessels using cones mounted on the agitator shaft at the liquid surface. Under gassed conditions and with surfactants added to the liquid, the spinning cone was shown to be effective in controlling the level and reducing the gas voidage over a wide range of operating conditions. The effectiveness of the cone as a defoamer appears to scale at equal tip speed suggesting that shear rate is dominant mechanism. Tests were done on a 2ft (0.61 m) and a 3ft (0.914 m) diameter stirred tanks

Keywords: Spinning cones, pumping rates, degassing, defoaming, level control, stirred tanks.

INTRODUCTION

Many industrial processes involve the introduction of gases to liquid systems or result in gaseous products through reaction, heat input or pressure reduction. Examples are oxidations, fermentations and hydrogenations. Equipment is used that is designed to maximise mass transfer and ease the separation of the component phases. The physical characteristics of these systems often result in the formation of foam, which can be problematic in terms of control and subsequent processing. Proprietary equipment, in the form of multiple spinning cones, is used in the food and related industries, for degassing foaming products. Other rotating mechanical devices, such as breaker bars, impellers and spinning discs, are also widely used for degassing foams in a wide range of industries. This work evaluates the effectiveness of a spinning cone as a degasser and potentially as a level control device in stirred tanks and hence its potential for adaptation in a wide range of industrial processes.

A hollow spinning cone fitted to the shaft of a stirred vessel, close to the operating level of the tank can act as a pump and reduce the gas hold-up. The cone picks up liquid from a pool at the inlet, accelerates it as a thin film up the walls and ejects it as a radial sheet at the top. Previous laboratory work using a foaming system indicated that the foam could be eliminated using a cone, with the foam level controlled at the cone outlet level. Under the same conditions without a spinning cone the contents foamed over the top. This suggested that the spinning cone might be a usefully employed to control level and foaming in industrial gas-liquid stirred tank applications. Also, since spinning cones have been used to intensify gas-liquid mass transfer [1-7] it is argued that the reduction in gas voidage could be done without detriment to the mass transfer operation.

A literature search indicates that foam reduction occurs mainly through the application of shear stress [9,10]. With a spinning cone this occurs at the wetted surfaces and from the radial sheet of liquid discharged from the top lip of the cone. The centrifuging action on the surface of the cone must also be a factor. Although many workers have studied the films on spinning cones, these were closed at the apex; therefore the film thickness measured was associated with a flow of liquid supplied to the cone surface by a separate pump. Hence, the literature indicated a knowledge gap regarding the spinning cone as a self-priming pump and could not tell us how to predict the pumping rates from the physical and geometric properties. A major aim of this work is to collect sufficient data to be able to fit it to a mathematical model describing the operation of the cone in terms of physical properties (cone speed; cone tip velocity; density, surface tension and viscosity of pumped liquid and geometrical properties (cone angle and shape of the cone surface).

LITERATURE REVIEW

Spinning cones are used commercially to intensify mass and heat transfer operations [1-8], for atomisation [11-17] and for shear spinning [18-20]. No papers that used of spinning cones as degassers were found, although they are used commercially for de-foaming vessel outlets, for example FUNDAFOM produced by Chemap AG of Switzerland. A number of papers have been published concerning the use of spinning "cups" as atomisers for agricultural sprays, slurries and molten metals. These generally focus on the form of the liquid film moving up the inside of the cups and the state of the fluid thrown from the cup periphery. As such there are some interesting results that are helpful from the viewpoint of understanding the experimental data.

The mechanism of foam break-up was explored by Goldberg and Rubin [9] who concluded that most mechanical processes for foam reduction consist basically of the application of shear stress. Tests were performed with foam discharged vertically onto a spinning disc and their results were compared with other methods of foam reduction such as liquid sprays, centrifugal, mechanical agitation or blowing through nozzles.

Hinze and Milborn [11] describe three basic processes that influence the form of a liquid film thrown from the rim of a spinning cone. For a cone rotating at a fixed angular velocity, these processes can be summarised as follows:

Disintegration by direct drop formation: At low pumping rates a liquid torus is formed close to the edge of the cone. The diameter of the torus is determined by the liquid properties

(density, viscosity and surface tension). External disturbances cause the torus to become varicosely deformed. Droplets are formed at the various bulges on the torus and are flung off by centripetal force.

Disintegration by ligament formation: At intermediate pumping rates, the bulges in the torus become more pronounced and the liquid leaves the cone in the form of thin jets or ligaments. If the pumping rate is gradually increased, the number of ligaments increases until a critical value is reached. If the pumping rate is increased further, the thickness of the ligaments increases but the number of ligaments remains constant. The ligaments flung from the cone are unstable and break up into drops some distance away from the edge of the cone.

Disintegration by film formation: The torus disappears at high pumping rates and a continuous sheet of liquid is flung from the edge of the cone. This sheet extends a small distance from the edge and then breaks chaotically into ligaments that in turn break into drops. Dombrowski and Lloyd [(12)] divide this mode of disintegration into two separate categories that they call "aerodynamic wave disintegration" and "turbulent disintegration". In the former the sheets break up into drops within a narrow radial band whereas in the latter disintegration takes place over a relatively large distance. From their experiments it appears that, for a given pumping rate, the break up category, either aerodynamic or turbulent, depends solely on the speed of the cone periphery.

The transition from disintegration by film formation to disintegration by ligament formation occurs when the following inequality is true

$$\left(\frac{Q}{D_C}\right)\left(\frac{r}{sD_C}\right)^{0.5}\left[ND_C\left(\frac{rD_C}{s}\right)^{0.5}\right]^{0.6}\left[\frac{m}{(r\,s\,D_C)^{0.5}}\right]^{0.167} < 0.442 \quad \textbf{Equation 1}$$

Similarly, the transition from disintegration by ligament formation to that by drop formation occurs when the following inequality is true

$$\left(\frac{Q}{D_C}\right)\left(\frac{r}{sD_C}\right)^{0.5}\left[ND_C\left(\frac{rD_C}{s}\right)^{0.5}\right]^{0.25}\left[\frac{m}{(r\,s\,D_C)^{0.5}}\right]^{0.167} < 2.88x10^{-3} \quad \textbf{Equation 2}$$

where Q is the pumping rate, D_C is the cone diameter, r is the fluid density, m is the fluid viscosity, s is the surface tension and N is the rotational speed of the spinning cone (rev/s).

The authors correlated the drop sizes measured in the various regimes**.** In the “aerodynamic wave regime” they obtained the following expression:

$$d_{32} = 0.742Q^{1/3}s^{1/3}m^{0.192}(v_S r^{1/6}) \quad \textbf{Equation 3}$$

where d_{32} is the volume-surface mean diameter and v_S is the velocity with which the liquid leaves the spinning cone. v_S is effectively equal to the velocity of the cone periphery ($2pNr$) except for liquids of low viscosity.

In the turbulent regime the data for oil and water was correlated separately:

$$d_{32} = 0.664\left(\frac{Q^{0.303}}{N^{1.36}D_C^{1.18}}\right) \text{(for water)} \quad \textbf{Equation 4}$$

$$d_{32} = 0.132\left(\frac{Q^{0.392}}{N^{1.27}D_C^{0.819}}\right) \text{(for oil)} \quad \textbf{Equation 5}$$

For ligament disintegration the result obtained was:

$$d_{32} = 0.0397\left(\frac{Q^{0.334}}{N^{1.32}D_C^{1.22}m^{0.1}}\right) \quad \textbf{Equation 6}$$

The impact of fluid viscosity on the drop size is an interesting feature of the above correlations. The effect of viscosity seems to depend on the mechanism of drop formation. For example, viscous liquids seem to give a smaller drop size than less viscous ones when disintegration goes via ligament formation but a larger drop size when a sheet is formed.

Hinze & Milborn [11], calculate the fluid flow within the cone using the following assumptions:

- The liquid layer thickness is small compared with the cone dimensions.
- The flow within the layer is viscous.
- The flow within the cone is rotationally symmetric.
- The static pressure across the liquid layer is constant
- The components of velocity normal to the surface of the cone and circumferentially around the cone are negligible compared with the component parallel to, and vertically up the cone surface. This implies that the path described by any liquid element with respect to the cone is practically straight and radial.

For the pumping rate (Q), the result is

$$Q = (2p/3m)\,r w^2 r^2 d^3 \sin f_C \quad \textbf{Equation 7}$$

where m = fluid viscosity; r = fluid density; w = angular velocity (rad.s^{-1}); r = radius of cone; d = film thickness; f_C = cone half angle. An alternative expression was suggested by Alan Jones [21]:

$$Q = 2pr^2\sqrt{\frac{wm\sin f_C}{r}} \quad \textbf{Equation 8}$$

where r is the large radius of the cone.

The mean radial velocity (v_{av}) is given by Hinze & Milborn [11] as:

$$v_{av} = \left(\frac{Q^2 r w^2 \sin f_C}{12 p^2 m r} \right)^{1/3} \quad \textbf{Equation 9}$$

A more recent paper by Makarytchev et al [22] gives an equation for the film thickness modelled as a wavy layer on top of a laminar sub-layer attached to the disc surface. The thickness of the film is an additive modification of the Nusselt model thickness $d^+ = d_N^+ + d_{wave}^+ = 0.91h^{2/3} + 1.95h^{-3}$, where h is a normalized radial distance. In the dimensional form, the proposed models express the film thickness and radial velocity as functions of cone geometrical and operating parameters. The authors maintain the validity of the models is consistent with independent velocity measurements on a rotating cone and film thickness measurements on rotating disks. However, h contains Q in the definition so like equation (7) cannot be resolved without knowledge of the flow rate.

Alcock and Froelich [15] calculate the energy balance for a spinning cone based on a unit mass flow Bernoulli equation and use this to predict the discharge velocity. The basic assumptions used are that:

- The change in internal energy of the fluid is negligible.
- The thermal energy input is zero.
- The potential energy change of the fluid on passing through the cone is negligible.
- The change in specific volume of the fluid is zero.

These give:

$$\frac{mP_1}{r} + \frac{v_1^2}{2} + W_S = \frac{mP_2}{r} + \frac{v_2^2}{2} \quad \textbf{Equation 10}$$

where v is the fluid velocity, W_S is the work input per unit mass and P is the pressure. The subscript 1 refers to the entrance to the cone and 2 the exit at the outer edge of the cone. Using this, the exit velocity is

$$v_2 = \sqrt{2(m/r)(P_1 - P_2) + v_1^2 + 2W_S} \quad \textbf{Equation 11}$$

The specific power W_S $(= W/Qr)$ where W is the power requirement and Q is the volumetric pumping rate can be related to the theoretical power requirement by expressing the torque (M) in terms of the momentum change ($M = m\Delta v$).

Thus, the theoretical power requirement is:

$$W_t = Qw^2 r \frac{(r_2^2 - r_1^2)}{2} \qquad \textbf{Equation 12}$$

and the specific power becomes:

$$W_S = w^2 \frac{(r_2^2 - r_1^2)}{2} \qquad \textbf{Equation 13}$$

Substituting this in the previous equation for v_2 and assuming that the first two terms are negligible, that is $v_1 << v_2$; $r_1 << r_2$ and $2(m/r)(P_1-P_2)$ is small – for example for water (m/r) = 1 x 10^{-6} m^2s^{-1} and $(P_1 - P_2)$ is typically of order 1-2 kPa) gives:

$$v_2 = wr_2 \qquad \textbf{Equation 14}$$

Therefore the tangential velocity reasonably approximates the fluid velocity at the edge of the cone.

The drop trajectories were calculated by Hashem [16] by assuming that the initial velocity of the drops is the same as the rim of the cone and that the drops are produced at the cone rim. The equations of motion used are:

$$a_z = -g - (3\rho_a C_d/4\rho_l d)|v|v_z \qquad \textbf{Equation 15}$$

$$a_x = - (3\rho_a C_d/4\rho_l d)|v|v_x \qquad \textbf{Equation 16}$$

where a = acceleration, C_d = drag coefficient = (24/Re)(1 + 0.1875Re + 0.00026Re^2), Re = drop Reynolds number = vdr/m, $v = (v_x + v_z)^{1/2}$ and d = drop diameter. The subscript z refers to the vertical direction, x to the horizontal, a to air and l to the liquid phase.

Given that the initial velocity of the drops is equal to the speed of the rim of the cone (that is $v_{x,0} = pND$) then, for a specified drop diameter, the equations of motion can be numerically integrated, once to give the drop velocity and twice to give the horizontal distance travelled for a given fall.

EXPERIMENTAL DETAILS

Experiments were carried out in mechanically agitated vessels and on a purpose built spinning cone rig designed to measure pumping rates.

THE STIRRED TANK RIGS

The schematic of the experimental rigs is illustrated in Figure 3. These consisted of two similar cylindrical mechanically agitated vessels each fitted with a quarter dish base. One was 0.61m inside diameter and the other was 0.91m. The cylindrical sections were fitted inside a square jacket through which water could be circulated for temperature control. The vessels were constructed from Perspex and the square jacket provided a distortion free viewing window for flow visualisation. Variable speed motors drove the shafts, and the

agitation speed was measured using Ferro-magnetic proximity sensors coupled to COMPACT MICRO 48 tachometers. The shaft power was measured using calibrated torque strain gauges bonded to the shafts. These strain gauges were wired to an ASTECH strain gauge bridge fitted with telemetry readout.

Gassing rates were measured using calibrated rotameters.

Temperature was monitored using thermocouples inserted through the analysis blocks.

The gas-liquid hold-up was estimated by level measurement of the aerated and unaerated vessel. Volumes were calculated ignoring the volume of the internals (shafts, agitators, cone and baffles.). Thus the gas hold-up was calculated from the calculated volumes estimated from the levels according to:

$$E_G = \left(\frac{V_G}{V_G + V_L} \right) x100\% \quad \textbf{Equation 17}$$

The vessel and agitator geometries are listed in Table 1.

		Vessel		
Vessel diameter	T (m)	0.61	0.61	0.914
Geometry key		1	2	2
Operating levels	H (m)	1.0	1.0	1.5
Agitator type	Bottom	A345	Radial turbine	Radial turbine
	Mid	A345	-	-
	Top	A345	PTB 6-blade 45° up	PTB 6-blade 45° up
Agitator diameters	D (all) (m)	0.292	0.305	0.305/0.457
Agitator clearances *(c)*	Bottom (m)	0.25	0.305	0.305
	Mid	0.5	-	-
	Top	0.75	0.5	0.5
Operating volume	V (dispersion) m^3	0.28	0.28	0.94

Table 1: Vessel and agitator geometries

Cones used were approximately $D_C = T/2$ with cones half angles of 30° and 15° on the 0.61m scale and 30° on the 0.914 m scale.

THE SPINNING CONE RIG TO MEASURE PUMPING RATES

Figure 4 is a schematic representation of the cone pumping rate rig. The cones used in the tests are listed in Table 2. The operating procedure was as follows

The motor rotated the shaft, onto which the hollow spinning cone was firmly affixed. Liquid was pumped into the trough (into which the cone was operating) from the reservoir. When the liquid started to immerse the cone, centripetal forces pumped a film of liquid up the cone's

surface to the top rim where it was discharged as a radial sheet of liquid over the sides of the trough. This liquid entered the reservoir to be recirculated. Eventually a steady state was reached where the rate at which liquid entered the trough from the reservoir equalled the rate at which the cone ejected liquid back into the reservoir. At that point the liquid flow rate shown on the rotameter equalled the pumping rate of the cone. At this equilibrium point, the height of the liquid and the liquid flow rate were noted.

Liquid heights and pumping rates were measured for a range of angular velocities, cone immersion depths and cone geometries. The effect of viscosity on pumping was tested using a glycerol solution. The effect of gas on pumping was tested by pumping the same fluid under gassed and ungassed conditions using the same geometry. In order to find the contribution of the inside and outside surfaces to the pumping rate, experiments were repeated with the inlet blocked allowing only material on the outside to be pumped.

Cone half angle	Cone material of construction	Outlet diameter of cone (D_C) m	Inlet diameter of cone (Di) m	Tested with inside blocked up?
15°	PVC	0.138	0.075	No
30°	Stainless Steel	0.180	0.050	No
30°	Stainless Steel	0.305	0.064	No
30°	PVC	0.142	0.025	Yes
45°	PVC	0.139	0.025	Yes
60°	PVC	0.144	0.025	Yes

Table 2: Cones used in pumping rate tests

SCOUTING EXPERIMENTS: REACTOR 2 (TABLE 1) GEOMETRY

An imperial standard 12" diameter stainless steel funnel (Figure 1) with a half angle of 30°, was adapted to fit the 0.61 m reactor 2 model. The gassing rate used in the test gave a superficial gas velocity of 0.11 m/s. A few ml of ASDA ULTRA washing up liquid had been added to the solution to cause severe foaming, so that without mechanical agitation, this gas rate caused the liquid to foam over the top of the cone. The level rapidly came under control when the agitator was switched on. The foam was dispelled with the level controlled at the top of the cone.

Flow visualisation showed that the cone picks up liquid from a pool at the inlet, accelerates it as a thin film up the walls and ejects it as a radial sheet at the top. This action destroyed the foam and gave a dramatic reduction in gas hold-up.

Questions that arose concerning the mechanism included:

Was the effect due to: *"g"* force (= ω^2 r/g)? Shear force? Do both inside and outside surfaces contribute? What is optimum cone angle? How does it scale up?

Effect of cone angle - tests with a 15° cone

To test whether "g" forces are the dominant parameter a 15° cone shown in Figure 1 was tested on the 0.61 m diameter reactor 2 model. This was not as effective as a degasser as the 30° at the same operating conditions. Compared with the no cone case, at a superficial gas velocity of 0.11 m/s and 10 "g" the 15° cone increased the liquid volume by 15% compared with a 20% increase in liquid volume when the 30° cone was used.

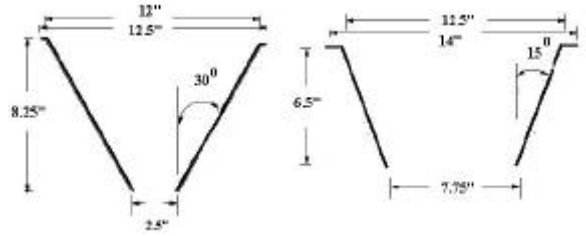

Figure 1: Cones used in scouting experiments in the 0.61m diameter vessel

CONE PUMPING RATE MEASUREMENTS

DISCUSSION

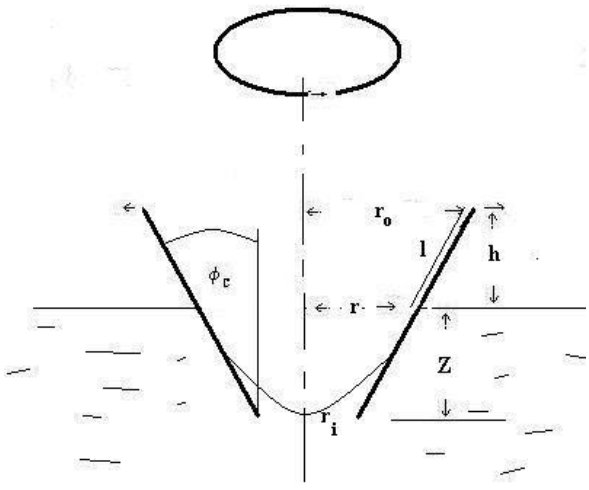

Figure 2:cone pumping considerations

Consider sketch: Cone of ½ angle f_C, inlet radius r_i and outlet radius r_o, immersed in pool of liquid to depth *Z*. When it is spun at speed *N* we can say:

- To spin liquid up from r then "*g*" (= w^2r/g) must be >1 at *r*
- To pump liquid down to r_i on inside of cone then "*g*" must be >1 at r_i.
- Velocity increases up the cone ∴film must thin up the cone or form rivulets (ligaments).
- To exit cone liquid rises through height *h* along length l.
- "*h*" and "*l*" are related via tan f_c.
- "*h*" is related to (r_o-r) via sin f_c.
- "r_i" is probably unimportant as long as liquid flow is not restricted.

EXPERIMENTS WITH CONES WITH AN HALF ANGLE OF 30°

Two 30° cones with outlet diameters D_C = 0.18 and 0.142m respectively and inlet diameters of 0.05m and 0.025m respectively were tested for a range of rotation speeds in water. The steady state immersion depths (*Z*) at different liquid supply rates (*Q*) were noted., *Q* was found to vary with the agitation speed^2 (N^2). By muliple regression it was found the data for the two sizes of cone could all be correlated as:

$$Q = 21.8" g_r " r^{1.37} (l/\min) \quad \textbf{Equation 18}$$

where *"g_r"* is *"g"* force at *r*

Correlation coefficient $R^2 = 0.91$

Equation 18 implies that the volumetric pumping rate is directly proportional to the applied "g" forces. The fit to the correlation is illustrated in Figure 5.

EFFECTS OF CONE ANGLE, GEOMETRY AND PHYSICAL PROPERTIES

A large number of experiments were carried out with a range of cone half angles from 15 to 60 degrees. Measurement of the immersion height was estimated to be accurate to 2 mm. Most of the tests were done with water but a number of runs were carried out with 75% by volume glycerol solution. This changed the viscosity and fluid density.

The results were analysed in dimensionless terms. Dimensionless groups considered were:

Dimensionless flow rate as:

- *Q/NV*, where *Q* = volumetric pumping rate, *N* = rotational speed and *V* = submerged volume of cone
- Q/NV_C, as (a) but V_C = total volume of cone

Cone half angle as the sine, cosine and tangent of fc.

Ratio of centripetal forces to gravitational forces *"g"* = *(wr/g)* with radius at *r* and r_o both tested.

Ratio of inertial to viscous forces as Tay number (cone Reynolds number) = rwr^2/m with radius at *r* and r_o both tested.

(r/r$_o$) ratio of radius cone radius at submergence level to cone radius at the top

(D_C/D_i) ratio of large cone diameter to inlet diameter.

Viscosity ratio as m/m_w, where m is the fluid vscosity and m_w is the viscosity of water at ambient temperature (20^0C).

After carrying out a large range of multiple regressions, it was found both *"g"* and Tay number gave better correlations when outlet values were used. Similarly cone volume V_C gave an improved fit to the submerged volume. It was also found that correlations could be obtained with similar R^2 coefficients involving both sine and tangent of f_C. When sin f_C was used, then the ratio D_C/D_i dropped out of the correlation without any significant change in R^2 regression coefficient. Examination of the fits showed that although tan f_C gave a good fit for 30° and 45° cones it gave a very poor prediction for 60° cones, over predicting some flow rates quite considerably. This did not show up on the correlation coefficient, as there are only a few points for 60° cones. Inclusion of the viscosity ratio improved the data fit.

The best overall fit with R^2=0.951 was:

$$\frac{Q}{"g"V_C N} = 155.6(\sin f_C)^{1.75} Tay^{-0.8} (r/r_o)^{2.5} (m/m_W)^{-0.5} \quad \textbf{Equation 19}$$

where, *"g"* and Tay are based on r_o and V_C is the total volume of the cone. The fit is illustrated in Figure 6.

TEST OF LITERATURE EQUATIONS

The equation proposed by Alan Jones (equation (8) [21], was tested against the experimental data. When *r* was taken as the large radius of the cone the equation did not fit. However, if *r* is taken as the radius of the cone at the submerged level it does give the right order of magnitude to the flow prediction and follows the trends although the fit is poor as illustrated by Figure 7.

To test for hydrodynamic effects on the data correlation, the data was split into separate sets obeying the literature criteria for transition to break-up from film to ligament formation as defined by equation (1) and (2). The majority of our data 119 points fell into the break-up from film disintegration. The fits to this data alone were worse (best correlation coefficient R^2 = 0.93) than for the entire data taken as one set. The smaller data set 35 points all fell into the break-up from ligament formation. This correlated better with an R^2 coefficient of 0.97. There was nothing to suggest however, that the 2 sets obeyed different scaling rules.

OPTIMUM CONE ANGLE

Equation (19) was used to predict pumping rates for a hypothetical range of cone ½ angles assuming a large diameter of cone *(D_C)* of 15 cm with an inlet diameter *(D_i)* of 5cm, spinning in water with immersion to D_C. This of course gives very long lengths of immersion for low ½ angles. The predicted pumping rates for cones of various angles rotated at 600 rpm are plotted against cone ½ angle in Figure 8. The curve shows a maximum pumping rate around a cone ½ angle of 40°, though the pumping rate is relatively insensitive to angle between 30° and 50°.

EFFECT OF AERATION ON PUMPING

Polypropylene glycol (PPG) (mol wt 2025) was used as a surfactant and ASDA ULTRA washing up liquid was used to induce foaming at levels of 10 parts per million (ppm). Back to back experiments were carried out with the same cone mounted in precisely the same position with water, water/PPG/soap and air-water/PPG/soap solution.

The comparisons of water with water/PPG/soap solution indicated that the change in surface tension did not unduly affect the pumping rate.

When the solution was aerated to give approximately 20% gas hold-up, the pumping rate of the cone did not change significantly. This is confirmed by a plot of flow rate/*"g"* against radius of immersion for the aerated soap solution and the ungassed water in Figure 9. Observations of the film suggested that only liquid was being pumped and that gas-liquid

disengagement is very rapid. Note however, that examination of the data set showed that all this data had been obtained at high *"g"* (>20 based on outlet flow). No similar comparisons have been made at *"g"* forces more realistic to large vessel operation.

CONTRIBUTION OF THE INTERNAL AND EXTERNAL CONE SURFACES TO PUMPING

In the cases where the inside of the cone was blocked up to ensure that all flow was up the outside of the cones, the pumping rate was approximately halved. In fact slightly more than a half was pumped, as the external diameter was greater than the internal. The pumping was found to be almost equally dependent upon the outside and the inside surface of the cones. Visually, this was a feasible conclusion to draw from examination of the rig when it was pumping with the inside blocked up. An example showing the 30° cone comparisons is given in Figure 10.

STIRRED TANK EXPERIMENTS

Tests were run on reactor geometry 2 using 20 ppm polypropylene glycol as a surfactant. With this geometry the reactor foamed quite badly when gassed without a cone. The 30° cone illustrated in Figure 1 was used in the tests. A gassing rate of 1980 l/min free air delivered was used for the tests, giving a superficial gas velocity of 0.11 m/s. Agitation rates were increased from 160 rpm to 300 rpm in steps of 20. The experimental data are plotted in Figure 11 in terms of gas hold-up against *"g"* force on the cone. When operated at the normal liquid level, the cone gave a significant reduction in gas hold-up compared to operation without a cone. The effectiveness levels off above about 10 *"g"* or a cone peripheral velocity around 4 m/s.

When similar tests were done with reactor (1) geometry, the tendency to foam was not as great. This is due to the proximity to the surface of the top agitator. Tests proved that much of the foam could be eliminated by operating with an agitator at a ½ to one agitator diameter from the dispersion surface, especially at high specific power inputs (>2W/kg). Even so typical reductions in gas hold-up of 10% were found for tests in 20-ppm PPG solution when the 30°, ½ angle cone was used. This cone was tested at operations up to a gas rate giving a superficial gas velocity of 0.87 m/s without flooding.

SCALE-UP

A solution of 8 ppm PPG and 10 ppm ASDA ULTRA washing up liquid was used for the tests. On the 0.61 m and 0.914 m diameter vessels tests showed that this solution foamed over when the cone was not fitted at the test gas superficial gas velocities of 0.07m/s.

Studies with the O.61 m vessel

A 12" diameter, 30° to the vertical cone pictured in Figure 1 was used in the 0.61m diameter tank for this work. Agitator geometry was that of reactor 1; see Table 1 and Figure 12. The cone was demonstrated to be effective between 240 rpm and 330 rpm at controlling foam due to a 10 ppm soap. Figures 13 to 15 illustrate the reduction in foam when the cone is switched on at 274 rpm. When the soap level was increased to 16 ppm, the cone was flooded at 274 rpm (Figure 16). The performance improved with increasing agitation speed. For controlling

the foam due to 16 ppm soap, we needed to operate at 390 rpm to match the 240rpm performance at 10 ppm soap. The *"g"* forces were varied from 10 to 26 with tip speeds between 3.8 to 6.2 m/s. At 274 rpm the tip speed was 4.4 m/s.

Studies with the 0.914 m vessel

On the 0.914 m vessel, the tests were done on an 18" diameter, 45° cone. Geometry was that of No 2 reactor (Table 1). The cone was demonstrated as effective for foam control between 150 rpm and 208 rpm for 10 ppm soap. Starting at 40 rpm the cone was completely flooded at the operational gas rate. Increasing agitation to 180 rpm quickly brought the level under control. Figure 17 captures a picture of the foam layer being reduced shortly after the agitation rate was increased. Conditions quickly stabilised at this speed with no splashing and the level reduced so that only an inch or so of foam was visible on the inside of the cone (Figure 18). By reducing speed in stages we found the cone could just control this foam down to speeds of 140 rpm. At 150 rpm it was quite stable (Figure 19) with a foam layer about 1/3 of the way up the cone. 140 rpm was verging on the edge of instability with foam occasionally spilling back into the cone (Figure 20). Below 140 rpm it started to flood. Increasing speed to 208 rpm did not cause any surface instability and the foam was well under control.

For the range of speeds from 150 to 208 rpm the *"g"* forces varied from 5.7 to 11 with tip speeds between 3.6 to 5.0 m/s. At 180 rpm (equivalent to operation at 274 rpm on the 0.61 m vessel scale) the tip speed was 4.3 m/s.

CONCLUSIONS

The use of a spinning cone for foam control and as a level control device is shown to work effectively up to the largest scale tested which was on a 3ft diameter vessel. Scaling at constant tip speed gave a very slight improvement with scale-up. This is certainly not due to the agitator geometry change, which had been shown to be detrimental on the 0.61m vessel work. It was probably due to the cone geometry change. Figure 8 indicates that a 45° ½ angle cone is more efficient at pumping than 30°.

POWER DRAW FOR SPINNING CONES.

The cone power P_C can be predicted from the Alcock and Froelich [15] equation (12).

$$P_C = Qw^2 r(r_o^2 - r_i^2)/2 \ (Watts)$$

Q is estimated from equation 19. We found good experimental agreement with equation (12) when the cone was operating with liquid level at the height of the top of the cone. For lower levels the power draw was lower. Power numbers for the cone varied from 0.2 when fully submerged down to 0.03 when the level is low.

NOMENCLATURE

C	Agitator clearance	m
D	Agitator diameter	m
E_G	Volume fraction of gas	
H	Height	m
m	Mass	kg
M	Torque	Nm
N	Agitation speed	s-1
NLL	Normal liquid level	m
P	Pressure	N/m^2
P_S	Shaft power	W
P_C	Cone power	W
P_0	Power number ($P_S/rN^3D^{5)}$	-
Q	Volumetric flow rate	m^3s-1
r_o	Outlet radius of cone	m
r_i	Inlet radius of cone	m
R	Radius of immersion	m
Re_a	Agitator Reynolds number ($\rho ND^2/\mu$)	-
T	Vessel diameter	m
Tay	Cone Reynolds number ($\rho\omega r^2/\mu$)	(-)
V	Volume	m^3
W	Power	W
v_s	Superficial gas velocity = Q/cross sectional area	ms-1
f	Angle to the vertical	
r	Density	kg/m^3
d	Film thickness	m
m	Viscosity	Pa.s
w	Angular velocity	rads/s
s	Surface tension	N/m
	SUBSCRIPTS	
C	Cone	
D	Dispersion	
I	Inlet	
L	Liquid	
U	Ungassed	
G	Gassed	
S	Specific	
t	Theoretical	
w	Water	

ABBREVIATIONS

PBT	Pitched blade turbine
ppm	Parts per million
PPG	Polypropylene glycol

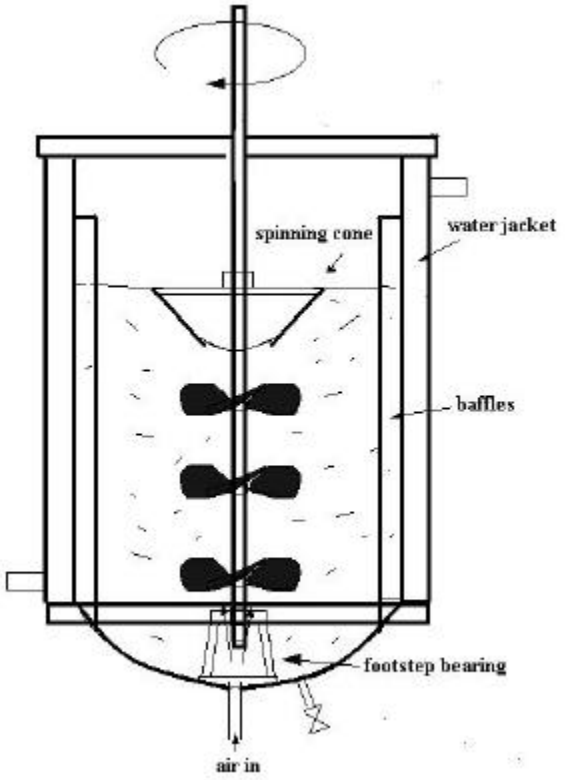

Figure 3: Stirred tank rigs

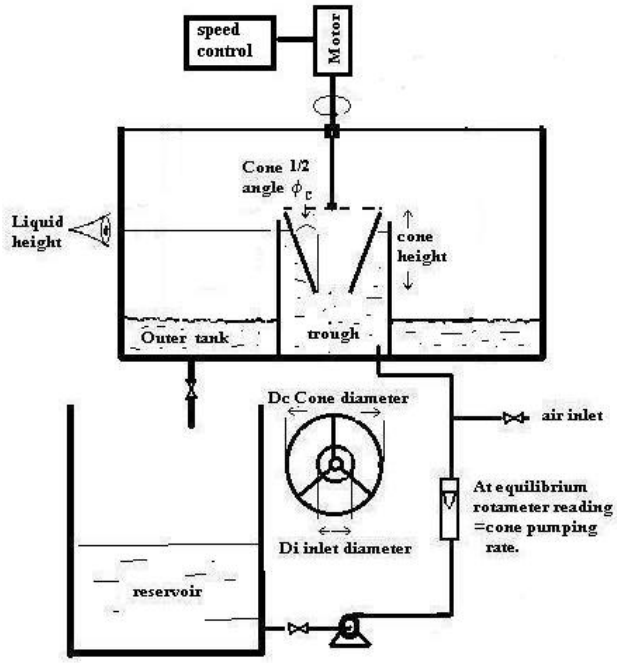

Figure 4:Cone pumping rate measuring rig

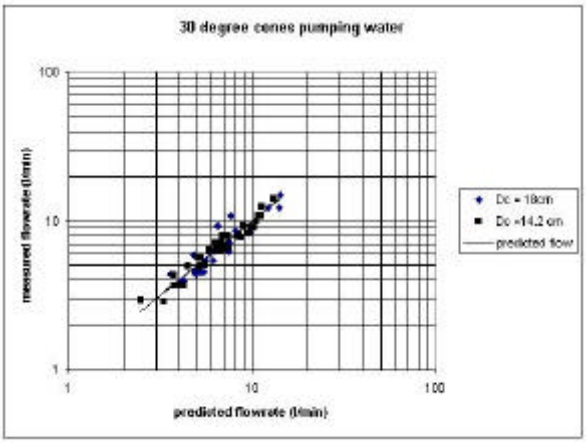

Figure 5:Data fit for 30^0cones to:

$$Q = 21.8"g_r"r^{1.37}(l/\min)$$

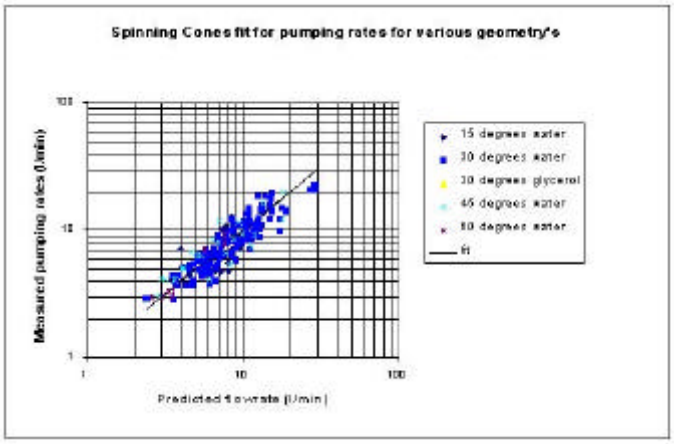

*

Figure 6: Data fit for all cones to:

$$\frac{Q}{"g"V_C N} = 155.6(\sin f_C)^{1.75} Tay^{-0.8} (r/r_o)^{2.5} (m/m_W)^{-0.5}$$

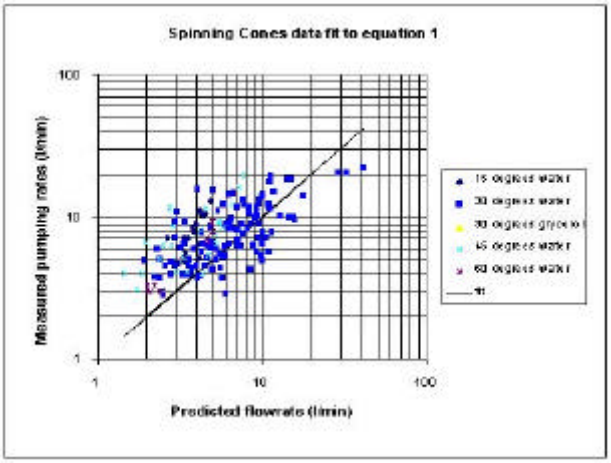

Figure 7: Pumping rate data fit to:

$$Q = 2pr^2\sqrt{\frac{wm\sin f_C}{r}}$$

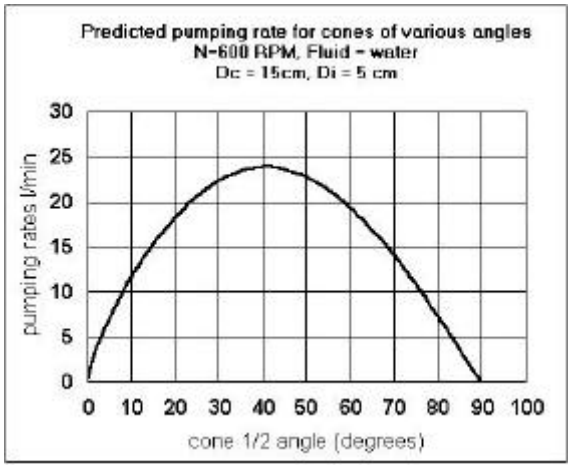

Figure 8: Optimum cone angle for pumping with fixed cone inlet and outlet diameters. Predicted using equation (19) and showing maxima at around 40°.

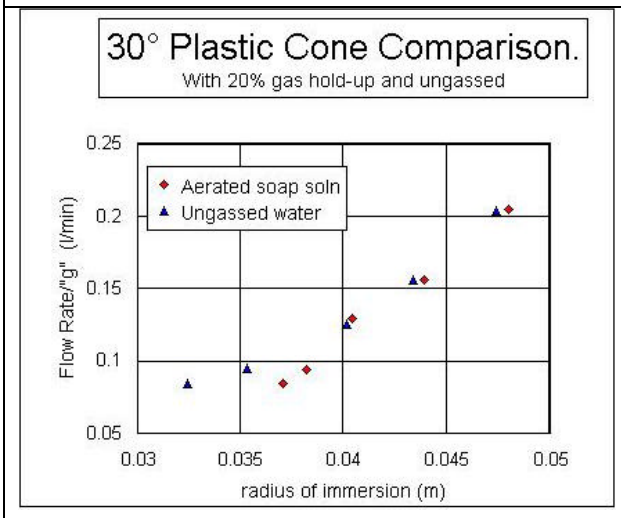

Figure 9: Affect of aeration and surfactants on the pumping rates of cones. Note these tests were done at "g" > 20 and have not been confirmed at lower "g".

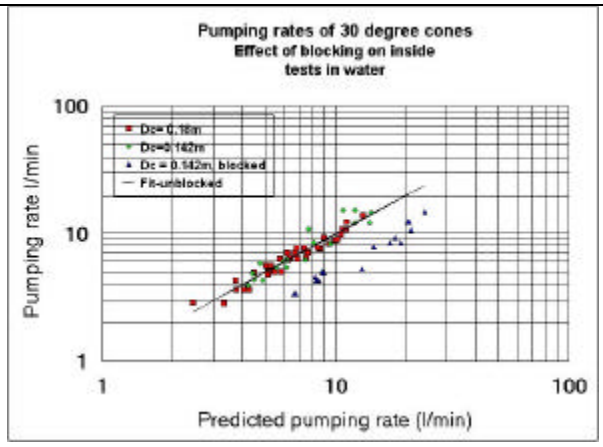

Figure 10: showing the effect of blocking up the inside of a 30° ½ angle cone. Flow is halved. Solid line is prediction from equation (18):

$$Q = 21.8"g_r"r^{1.37}(l/\min)$$

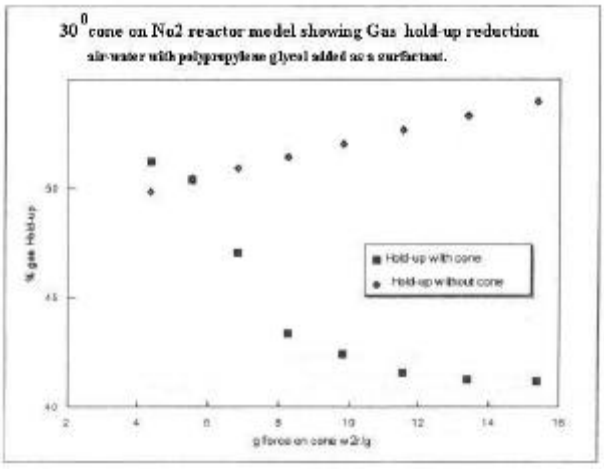

Figure 11:reduction in gas hold-up using a 30° cone.

Figure 12:A345 agitators with the 30° cone

Figure 13: 0.61m vessel. Cone flooded, agitator switched on to bring foam under control. 10 ppm soap

Figure 14:Level coming under control, 0.61m vessel 274 rpm, 10 ppm soap.

Figure 15: 0.61m vessel, 274 rpm, and 10 ppm soap. Level completely under control

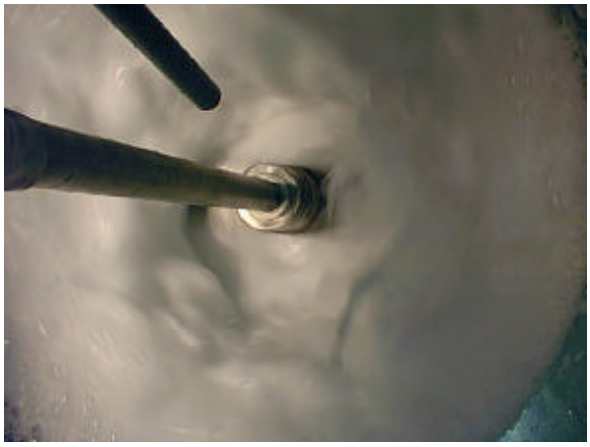

Figure 16: 0.61m tank, 274 rpm, soap increased to 16-ppm. Cone flooded

Figure 17: 0.914m vessel. Reducing foam at 180 rpm after complete foam-out at 40 rpm.

Figure 18: 0.914m vessel. Equilibrium foam at 180 rpm.

Figure 19: 0.914m vessel. Stable operation at 150 rpm

Figure 20: 0.914m vessel. Just coping with foam at 140 rpm

REFERENCES

1. Prince, R. G. H.; Desho, S.; Langrish, T. A. G. (1997), "Spinning cone column capacity and mass transfer performance Inst. Chem. Eng. Symp3329999. Series 142 (Distillation and Absorption '97, Vol. 2), pp. 769-781.
2. Zivdar, M.; Langrish, T. A. G.; Prince, R. G. H. (2001), "Comparison of mass-transfer efficiencies of SCC and structured packing". Int. J. Eng. Vol.14(1), pp. 1-8.
3. Sykes, S. J.; Prince, R. G. H. (1992), "The design of spinning cone distillation columns". Inst. Chem. Eng. Symp. Ser. 128 (Distillation and Absorption '92, Vol. 1), pp. A167-A179.
4. Middleton, J. C. (1997), "Applicability of high-intensity gas-liquid reactors to typical chemical processes". BHR Group Conf. Ser. Publ. Vol. 28 (Process Intensification in Practice), pp.135-142.
5. Wright, A. J. and Pyle, D. L. "Extractive fermentation and the spinning cone column: preliminary studies". IChemE Res. Event--Eur. Conf. Young Res. Chem. Eng., 1st (1995), 2 998-1000
6. Badcock, R.J.; Benwell, R. A.; Gray, C. (1994). "An evaluation of spinning cone column technology for low alcohol beer production". Proc. Conv. - Inst. Brew. (Asia Pac. Sect.) 23rd pp.170-175.
7. Vallet, L. (1980), "Thin film evaporation for the removal of solvents". Engl. Editor(s): Curling, John M., Methods Plasma Protein Fractionation pp. 211-22. Publisher: Academic, London, Engl
8. Vira, N. R.; Fan, Dah Nien. (1981), "Heat transfer from a cone spinning in a corotating fluid". J. Heat Transfer Vol.103(4), pp. 815-817.
9. Goldberg M, and Rubin, E. (1967) "Mechanical foam breaking" Ind. Eng. Chem. Process. Des. Dev., vol. 6 pp. 195-199.
10. Gutwald, S. and Mersmann A. (1997) "Mechanical foam breaking – A physical model for impact effect with high speed rotors." Chem. Eng. Technol., Vol. 20, pp 76-84.

11. Hinze, J.O. and Milborn, H, (1950), “Atomisation of liquids by means of a rotating cup”. J. App. Mech., Vol.17, pp. 145-153
12. Dombrowski, N. and Lloyd, T.L. (1974) “Atomisation of liquids by means of a spinning cup” Chem. Eng. Journal, 8 (1974) 63
13. Dombrowski, N.; Lloyd, T. L., Appl.Sci.Res., 28 (1973) 278
14. Dombrowski, N.; Lloyd, T. L. (1973), “Air drag on ligaments produced from rotating cups”. J. Chem. Eng. Jap. Vol. 6(4), pp. 363-365.
15. Alcock, R. and Froelich, D. (1986), Trans. ASAE, 26 1514
16. Hashem, A. (1991), Appl. Eng. Agric., 7 305
17. Eisner, A. D. and Martonen, T. B. (1988), “Simultaneous production of two monodisperse aerosols using a spinning-top aerosol generator”. Aerosol Sci. Technol. Vol. 9(2), pp. 105-113.
18. Sernka, Richard P.; Ledman, John L. (1969), “Development of shear spinning technology for beryllium”. U. S. At. Energy Comm. (SC-R-69-1233), 34 pp. From: Nucl. Sci. Abstr. 1969, 23(15), 29985.
19. Straub, Curt; Hailey, Robert W. (1966), “Spinning of refractory metals”. Metall. Soc. Conf. [Proc.] 30 pp. 423-431.
20. Rose, Charles H. and Watervliet Arsenal, (1966), “Application of shear-spinning techniques in forming molybdenum missile components”. U. S. C. F. S. T. I., AD Rep. (1966), (AD 631423), 29 pp. From: U.S. Govt. Res. Develop. Rept. 41(11), 53.
21. Jones Alan, F., (1996) Manchester University Maths Dept. Private Communication
22. Makarytchev, S. V.; Langrish, T. A. G.; Prince, R. G. H. (2001), “Thickness and velocity of wavy liquid films on rotating conical surfaces”. Chem. Eng. Sci 56(1), pp.77-87
23. Hall, P., Sedney, R. and Gerber, N. (1990), “Dynamics of the fluid in a spinning coning cylinder”. AIAA J vol. 28(5), pp. 828-835.
24. Langrish. T. A. G.; Prince, R. G. H.; Messner, S.; Sykes, S.; Meldrum, A. L. (1993), “The flow of liquid in spinning cone columns”. Off. Proc. Comb. Conf., 6th Conf. Asia Pac. Confed. Chem. Eng., 21st Australas. Chem. Eng. Conf. 2 13/2-17/2

AKNOWLEGEMENTS

The authors would like to acknowledge to contribution of Simon Lee who collected much of the cone pumping rate data in the summer of 1996 and also ICI Technology (ICI Research and Technology Centre, UK), Huntsman Polyurethanes (3078 Everburg, Belgium) and DuPont (UK) Limited (DuPont Polyester Technologies), who supported this work.